Combined Wind and Waves over a Fringing Reef

Alejandro Sánchez, Jane McKee Smith, Zeki Demirbilek, and Stan Boc

Coastal Hydraulics Laboratory, U.S. Army Corps of Engineers, Vicksburg MS

1. Introduction

Tropical islands may encounter strong wave and wind events due to tropical cyclones which cause severe damage and life-threatening conditions. The capability to quickly forecast the coastal wind and wave conditions for estimating the resulting coastal inundation is crucial for planners and decision-makers responsible for early warnings, evacuations and relief procedures (Cheung et al. 2003). Protective coastal structures are commonly designed using hindcast wave and water levels and/or simulating a large number of hypothetical cyclones representative of historical events (e.g. Thompson and Scheffner, 2002).

One of the challenges in estimating storm-induced coastal inundation is the prediction of the nearshore waves. This requires using nonlinear wave models such as Boussinesq-type models to obtain accurate estimate of waves. These two-dimensional (2-D) fully nonlinear models are computationally demanding. An alternative is to use simpler 1-D models to simulate wave transformation over several transects along the coastlines that are of concern for flood innundation. Nwogu (2006) was able to obtain similar wave runup using 1-D and 2-D Boussinesq wave model simulations of nearshore waves during Hurricane Iniki along the coast in Kauai, Hawaii. The 1-D models have been used extensively and successfully in calculating waves in the surf zone (e.g., Gerritsen 1980; Thornton and Guza 1983; Dally et al. 1985; Dally 1992; Larson and Kraus 1992; Massel and Brinkman 2001), bottom morphology changes (e.g., Van Rijn et al. 2003) and currents (e.g., Thornton and Guza 1986; Ruessink et al. 2001; Gourlay 2005).

Over the past decade, the Coastal and Hydraulics Laboratory (CHL) of the U.S. Army Engineer Research and Development Center (ERDC), has developed and improved numerical modeling procedures for determining coastal waves and inundation for tropical storms (e.g., Thompson and Scheffner, 2002; Demirbilek et al. 2007a; Demirbilek and Nwogu 2007b). The Surge and Wave Island Modeling Studies (SWIMS) project of the US Army Corps of Engineers (USACE) is developing predictive capabilities for island flood estimates. One of these tools is a simple, first-order, integrated wave

modeling package, called TWAVE (Sánchez et al. 2007). TWAVE is intended for the US civil defense agencies and USACE District Offices, providing users a practice-oriented package which is user-friendly, flexible and robust and suitable for the feasibility and reconnaissance type engineering planning studies.

In this paper, the focus is on wave transformation over fringing reefs and potential effects of wind on reef-top dynamics. In the first section, measurements from two laboratory studies of wave transformation and setup over fringing reefs are discussed. In the second section, existing empirical and semi-analytical formulations for estimating wave setup over a fringing reef are reviewed. Revised equations are proposed that include the contribution of wind setup. The numerical models results are compared with laboratory measurements of wave heights, mean water levels and runup in the third section of this paper. Conclusions and recommendations are provided at the end of paper.

2.0 Laboratory Datasets

2.1 University of Michigan Dataset

The first experimental dataset use in this study is that of Demirbilek et al. (2007a). These experiments consist of approximately 80 test carried out on a 1:64 scale model of a fringing reef type profile in a wind-wave flume at the University of Michigan (UM). The reef profile is similar to that of Seelig (1983) except it does not include a reef lagoon (Figure 1). A similar profile was also used by and Thompson et al. (2005) that had a more narrow reef width. Reefs with a flat reef top are common in the Southern coast of the Island of Guam. The flume is 35 m long, 0.7 m wide and 1.6 m high. Random unidirectional waves were generated using a plunger type wave maker and winds were generated using a 40-horsepower blower capable of producing winds up to 30 m/sec. The instrumentation consisted of nine capacitance-wire gauges to measure wave and water surface elevations along the reef profile, one 1-m-long capacitance-wire runup gauge, and two anemometers for the wind speeds. The significant wave height was calculated using $H_s = 4\sqrt{m_o}$ where m_o is the integration of the water surface spectral density over frequencies smaller than infragravity waves (<0.04 Hz). This data set is referred to hereafter as the UM dataset.

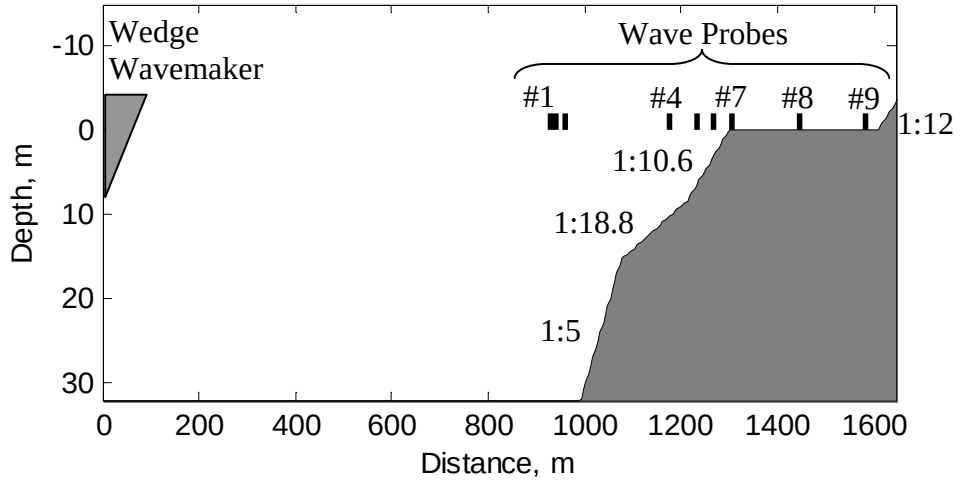

Figure 1. Experimental setup for UM fringing reef experiments. Dimensions are in prototype scale. Depth is with reference to reef-top

The deepwater wave steepness, defined as H_o / L_o where H_o and L_o are the deep water significant wave height and wave length respectively, in the UM dataset varied between 0.015-0.05. The laboratory results were scaled up to prototype scale of 1:64 using the Froude scaling. The bottom friction and wind drag coefficients were not scaled. Since the experiments were carried out over smooth bottoms, the bottom friction was considered to be negligible. The wind drag coefficient was calibrated by adjusting its value to fit laboratory measurements from tests which had no paddle generated waves (wind only testa). In the numerical study presented here, STWAVE and ADCIRC models were used to obtain a linear function of the drag coefficient as a function of the wind speed. Nonetheless, even the wind-only test cases generated waves that contributed to the wave setup over the reef. Therefore, the calibrated drag coefficients might be slightly overestimated.

2.2 Hayman Island Dataset

The second laboratory dataset was obtained from the monochromatic wave experiments conducted by Gourlay (1994) for an idealized fringing reef profile similar to those found in the southern side of Hayman Island, North Queensland Australia (Figure 2). The dataset consists of 18 tests of regular waves with 1-3.5 m heights, 3.8-6.8 sec periods, and a deepwater wave steepness of approximately 0.048. The water depth over the reef varied from 1.4 m to 3.4 m.

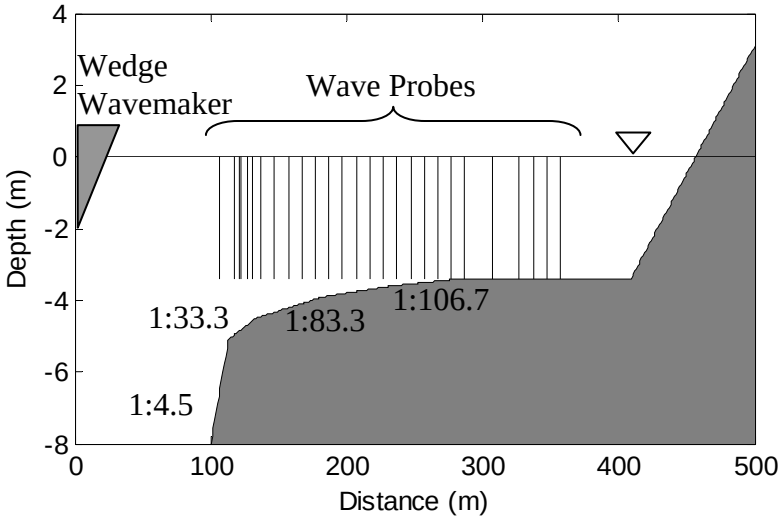

Figure 2. Experimental setup for Hayman Island fringing reef experiments. Dimensions are in prototype scale.

3.0 Empirical Relations

3.1 Waves Setup

Seelig (1983) obtained the following empirical relation for wave setup by using laboratory experiments for a fringing reef profile similar to the one used in the UM experiments. He related the wave setup to a parameter resembling the wave power as:

$$\Delta\eta = \begin{cases} -0.92 + 0.77\log_{10}\left(H_o^2 T\right) & \text{for } h_r = 0 \text{ m} \\ -1.25 + 0.73\log_{10}\left(H_o^2 T\right) & \text{for } h_r = 2 \text{ m} \end{cases} \quad (1)$$

where T is the wave period, H_o is the deepwater wave height and h_r is the still water depth over the reef. One of the disadvantages of Equation 1 is that it is only valid for depths 0 and 2 m. To obtain the wave setup at water depths other than 0 and 2 m, the setup is usually interpolated. We should note that Equation (1) can produce negative values of wave setup for small wave heights and periods.

Gourlay (1996a) investigated wave setup and wave-generated current over reefs using physical modeling experiments for idealized fringing and platform reefs. He determined that the setup increased with both increasing wave heights and period, and decreased with increasing depth over the reef top. Using a wave energy balance equation, Gourlay (1996b) obtained an implicit solution for wave setup.

$$\Delta\eta = \frac{3}{64\pi} K_p \frac{g^{1/2} H_o^2 T}{\left(h_r + \Delta\eta\right)^{3/2}} \left[1 - K_R^2 - 4\pi K_r^2 \frac{1}{T} \sqrt{\frac{h_r + \Delta\eta}{g}} \right] \quad (2)$$

where K_p is a shape factor which accounts for the effects various dissipation mechanisms over the entire reef profile, K_R is a wave reflection factor, K_r is a wave transmission factor and g is the gravitational constant. This relation has been used successfully for predicting wave setup on reefs with steep faces by Gourlay (1996b, 1997). The *K* factors in Equation 2 must be calibrated for each reef profile. As pointed out by Gourlay (1996b), the factors appearing in Equation 2 are not necessarily constant for different reef profiles. The shape factor for example is expected to be a function of the still-water depth and offshore wave height and period, since these will determine the segment of reef (bathymetry) over which the waves will break. Because the bottom friction is not included, Equation 2 is not expected to be accurate for wide, shallow reefs with rough bottoms (Gourlay 1996b).

The first term in Equation 1 is related to the still-water depth (SWL) and the second to the offshore wave energy. The setup increases as the SWL over the reef decreases (Gerritsen 1980, Gourlay 1996ab, Gourlay 2005). The setup is also related to the offshore wave steepness (Gerritsen, 1980), therefore we provide a expression similar to that of Seelig (1983):

$$\Delta\eta_{wave} = -0.18 h_r + 0.48 \log_{10}\left(H_o^2 T\right) - 5.53 H_o / T^2 \quad (3)$$

Equation 3 along with Seelig's and Gourlay's equations are compared to the measured setup over the reef top in Figure 3. One of the problems with Seelig's empirical formulation is that it can lead to negative wave setup values for small wave height conditions. Gourlay's equation was calibrated by assuming that the wave reflection is negligible (K_R=0) and adjusting K_p to match the measurements. Demirbilek et al. (2007a) calculated reflection coefficients for the wind-wave flume experiments of less than 10%. According to Gourlay (1996b), the wave reflection does not have a significant effect on wave setup when the reflection coefficient is less than 20%.

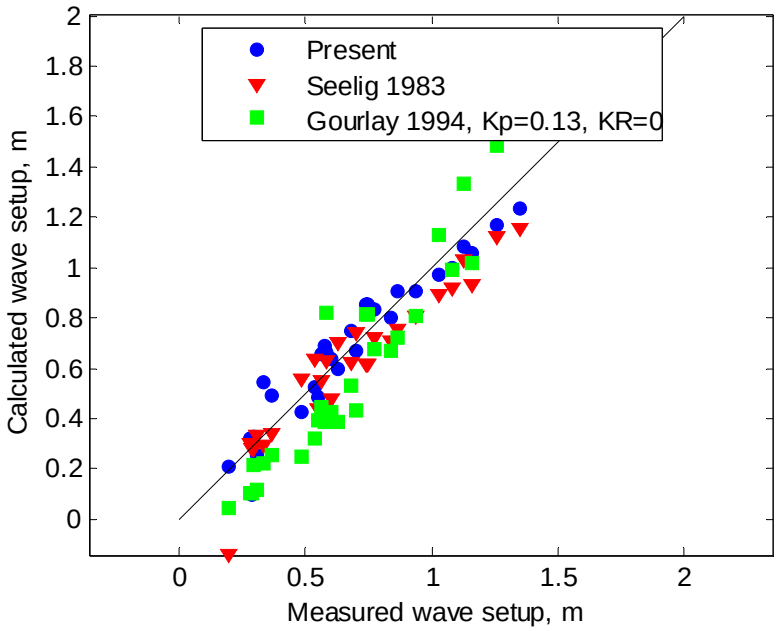

Figure 3. Comparison of measured (UM dataset) and computed wave-setup using Seelig (1983), Gourlay (1994) and a modified form of Seelig's equation.

Equation 3 shows improved results compared to both Seelig's and Gourlay's formulations for the UM dataset. Equation 3 also does not produce negative setup values. Although Equation 3 does not have any free calibration parameters, the empirical constants are expected to be a function of the reef geometry, and therefore Equation 3 is only valid for fringing reef type profiles.

3.2 Wind Setup

The above results show that it is important to consider the wind setup in empirical estimates of water levels over a fringing reef. The following empirical relation, which is based on the momentum balance of wind stress and water surface gradient provides a simple expression to estimate the wind contribution to the setup over a fringing reef:

$$\Delta\eta_{wind} = \frac{WC_d U^2}{K(h_r + \Delta\eta_{wave})} \tag{4}$$

where W is the width of the reef top in meters, C_d is the wind drag coefficient, U is the wind speed in m/sec, K is an empirical coefficient, and h_r is the still-water depth over the reef top in meters and $\Delta\eta_{wave}$ is the wave setup calculated using Equation 3. The total water level over the reef top is then $\Delta\eta_{total} = \Delta\eta_{wave} + \Delta\eta_{wind}$. The coefficient K in the denominator of Equation 4 was found by minimizing the root-mean-squared error

(RMSE), however the results are not sensitive to this parameter and reasonable results were found for values of K between 800,000 and 120,000.

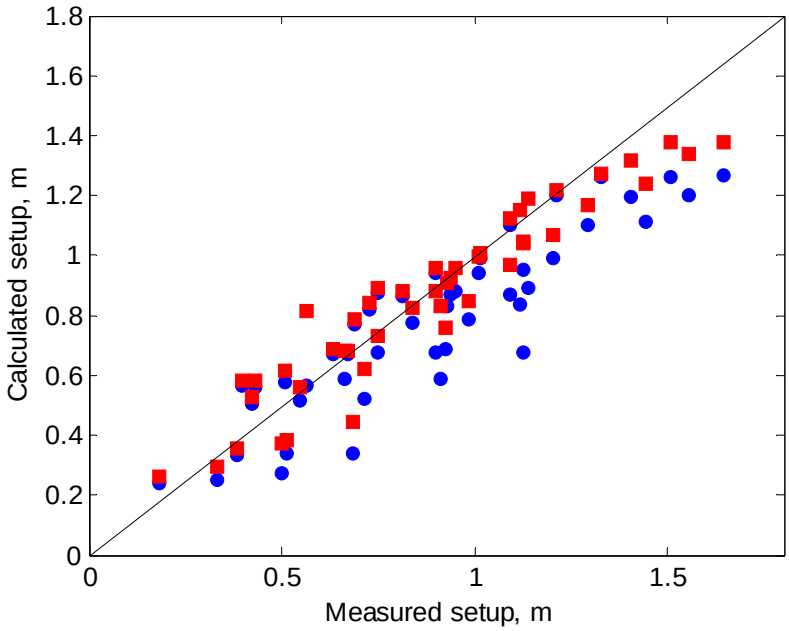

Figure 4. Comparison of measured (UM dataset) and calculated setup over the reef top. ● Only wave setup (Equation 3); ■ Wind and Wave setup (Equations 3 and 4)

It is noted that both empirical Equations (3) and (4) were obtained from the UM dataset. These empirical formulas are applicable only to fringing reef profiles with steep faces. Additional validation data are required to determine the applicability of these proposed formulas to other reef geometries different than that of Guam used in the UM experiments.

4.0 Numerical Models

4.1 STWAVE and ADCIRC

The STeady-state spectral WAVE (STWAVE) model (Smith et al. 2001) was used to transform waves over the reef. The ADvanced CIRCulation (ADCIRC) model (Luettich et al. 1992) was used for water level estimates over the reef. STWAVE was run using a 5-m grid resolution. ADCIRC was run using a 10- to 30-m variable resolution grid and a time-step of 0.2 sec until steady-state conditions were achieved. A two-way coupling between the models was performed by passing the wave radiation stress gradients from STWAVE to ADCIRC and then re-running STWAVE with adjusted depths to account for

the mean water surface elevations from ADCIRC. This process was repeated at least one time and then STWAVE was re-run a final time. For these tests, the wave breaking was modified in STWAVE to apply the Battjes and Jannsen (1978) formulation given by

$$D_b = \frac{1}{4}\rho g B \bar{f} H_b^2 Q_b \tag{5}$$

where D_b is the energy dissipation per unit area, ρ is water density, B is the wave breaking intensity factor (set to 1.0), $\bar{f}$ is the wave frequency, H_{rms} is the root-mean-square (rms) wave height, d is the total water depth and Q_b is the fraction of broken waves given by the implicit relation $H_{rms}^2 \ln Q_b = H_b^2(1-Q_b)$. For steep slopes this formulation does not produce enough wave dissipation to counter wave shoaling (Jannsen and Battjes 2007). To remediate this, the significant wave height was limited to the breaking wave height given by Miche's criterion (1951) $H_b = 0.88\tanh(kd)/k$, where k is the wave number.

The finite element circulation model ADCIRC was forced with the wave radiation stress gradients from STWAVE and wind stress $\tau_{wx} = C_d \rho_a U |U|$ where ρ_a is the air density, C_d is the wind drag coefficient and U is the average wind speed measured in the flume. The wind drag coefficient was calibrated by matching the computed wind setup with measured setup for the tests which had no waves or very small waves. For brevity, the coupled STWAVE and ADCIRC modeling system will be hereafter referred to as STAD.

4.2 One-Dimensional Wave Energy Balance Model

With the assumption of alongshore uniformity in the bathymetry, the time-averaged wave energy balance equation becomes

$$\frac{\partial}{\partial x}(EC_g \cos\theta) + D_b + D_f = 0 \tag{6}$$

where E is the wave energy per unit area, C_g is the wave group velocity, θ is the wave incidence angle, D_b and D_f are the wave energy dissipation due to breaking and bottom friction respectively. Since the laboratory tests were conducted over a smooth surface, the friction is considered to be negligible and set to zero.

Two types of formulations were used to estimate the breaking wave dissipation. The first is the empirical model of Dally et al. (1985) is expressed as

$$D_b = \frac{\kappa}{d}\left[EC_g - \min(E, E_s)C_g\right] \tag{7}$$

where κ is an empirical decay coefficient and E_s is the stable wave height energy equal to

$$E_s = \frac{1}{8}\rho g(\Gamma d)^2 \tag{8}$$

where Γ defines the stable wave height are percentage of the water depth. Following Smith et al. (1993), we adapted 0.15 and 0.42 for the values of κ and Γ. This approach has successfully used in modeling wave transformation over irregular bathymetry including reefs (e.g., Gerritsen 1980, Dally 1992). Assuming that the waves follow a Rayleigh distribution

$$p(H) = \frac{2H}{H_{rms}} \exp\left[-\left(\frac{H}{H_{rms}} \right)^2 \right], \tag{9}$$

the root-mean-squared (rms) wave height can be obtained from

$$E = \frac{1}{8}\rho g \int_0^\infty H^2 p(H) dH = \frac{1}{8}\rho g H_{rms}^2 \tag{10}$$

and is related to the significant wave height by $H_s = \sqrt{2} H_{rms}$.

It is important to mention that Equation 7 does not depend on the chosen wave height distribution. The wave height distribution is only used to obtain a characteristic wave height from the wave energy. This means that Equation 7 can be used for both random and monochromatic waves.

The second formulation adopted for wave breaking dissipation was based on the early work of Battjes and Janssen (1978). Recently, Alsina and Baldock (2007) and Janssen and Battjes (2007) separately obtained the following expression for wave breaking dissipation for an unsaturated surf zone as

$$D_b = \frac{3\sqrt{\pi}}{16}\rho g B \bar{f} \frac{H_{rms}^3}{d} Q_b \tag{11}$$

where the fraction of broken waves is equal to

$$Q_b = 1 + \frac{4}{3\sqrt{\pi}} \left(R^3 + \frac{3}{2} R \right) \exp\left(-R^2 \right) - \mathrm{erf}(R) \tag{12}$$

In Equation 12, erf is the error function and $R = H_b / H_{rms}$. The breaking wave height is obtained from $H_b = 0.88 \tanh(\gamma k d / 0.88)/k$, where, the breaker index is calculated as in Alsina and Baldock (2007) using the expression of Battjes and Stive (1985) $\gamma = H_b / d = 0.5 + 0.4 \tanh(33 H_o / L_o)$. Equation 11 is obtained by following a similar

approach as in Battjes and Janssen (1978) except that rather then assuming a clipped Rayleigh distribution, a complete Rayleigh distribution has been assumed.

4.3 Momentum balance over a reef

Assuming uniformity in the alongshore direction (y-direction) and ignoring mixing and cross-shore currents, the time-averaged and depth-integrated 1D momentum equation may be written as

$$\rho g(h+\eta)\frac{\partial \eta}{\partial x}+\frac{\partial S_{xx}}{\partial x}=\tau_{wx} \tag{13}$$

where η is the wave setup relative to still-water level, h is the still-water depth relative to a specific vertical datum, and S_{xx} is the wave radiation stress in the x-direction and τ_{wx} is the wind stress in the x-direction. The wave radiation stress is approximated using linear wave theory for an arbitrary wave angle as (Longuet-Higgins and Stewart 1964) as $S_{xx}=E(n(\cos^2\theta+1)-0.5)$ where θ is the incident wave angle and $n=0.5\left[1+2kd/\sinh(2kd)\right]$. Equations 6 and 13 are solved simultaneously from deep to shallow water. When the formulation for wave breaking of Dally et al. (1985) is used in the calculations, the model is referred hereafter as DDD85, and when the formulations of Alsina and Baldock (2007) and Janssen and Battjes (2007) are used, the model is designated by ASJB07.

5.0 Comparison of Models with the UM Data

The STAD, ABJB07 and DDD85 models are compared with the UM laboratory measurements. The effects of wind on wave transformation and setup are shown for subsets of the laboratory measurements.

5.1 Waves Only Tests

Figure 5 shows an example of measurements and computed significant wave heights and mean water surface elevation for Tests 17 and 47 which were forced only with waves (Demirbilek et al. 2007a). Gauge 4 (fourth measurement station from left end of the flume) shows an obvious bias due to problems with the gauge (Demirbilek et al. 2007a) but is included here for completeness. Wave setup is slightly underestimated by STAD over the reef top. Significant wave height values are larger than measurements and those obtained from ABJB07. The ABJB07 and DDD85 models predicted similar mean water levels that are in good agreement with measured values. The STAD and ABJB07 models have similar wave breaking parameterizations that produced nearly the same wave

heights except over the reef top where STAD produced slightly higher wave heights. The largest difference between DDD85 and the other models is in the energy dissipation , which tends to zero once the wave height has reached its stable value. Consequently, this would cause an overprediction of wave heights at the Gauges 8 and 9 for two test conditions shown in Figure 5. DDD85 also predicts comparatively higher breaking wave heights than the other two models.

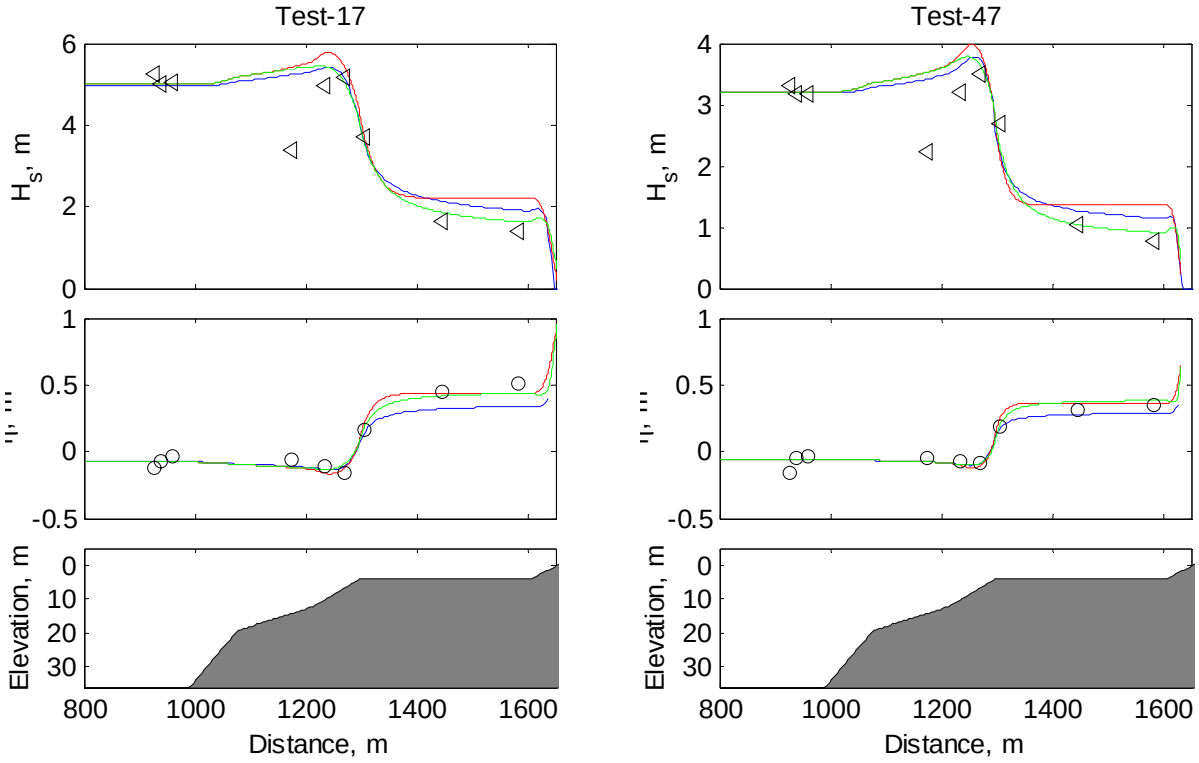

Figure 5. Comparison between measured and computed significant wave heights and mean water levels for Test 17 (H_o =4.99 m, T_p =12.0 sec, h_r =3.26 m, U =0.5 m/s) and Test 47 (H_o =3.20 m, T_p =12.0 sec, h_r =1.92 m, U =0.7 m/s).

— ABJB07, — DDD85, — STAD.

Figure 6a shows the calculated versus measured significant wave heights for all the tests which were forced with only waves using STAD. This approach predicts well the wave heights up to Gauge 6 (just before reef rim) and underestimates wave heights at Gauge 7. A possible cause of the underestimation is the wave breaking formulation. Gauge 4 data points to instrumentation problems (Demirbilek et al. 2007a). The measured and STAD calculated water surface elevations are compared in Figure 6b. There is a significant

underestimation of the both the wave setdown (Gauges 5-6) and setup (Gauges 7-9). In addition, the wave setup is limited to 0.4 m over the reef.

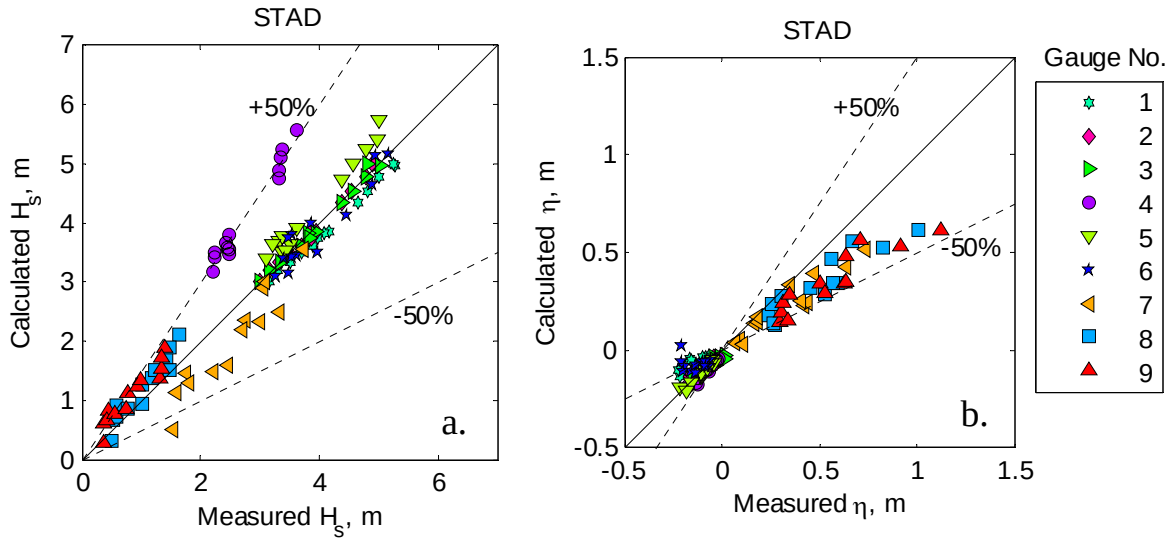

Figure 6. Comparison between measured and calculated significant wave heights and average water levels for the events with only wind using STAD.

The measured and ABJB07 model calculated significant wave heights are shown in Figure 7a. The agreement is good at all gauges (discarding gauge 4 data for reasons previously stated). The measured and ABJB07 model calculated surface elevations are compared in Figure 7b. Predicted wave setup over the reef top is within 50% of the measured values, and wave setdown at Gauges 5 and 6 are underestimated.

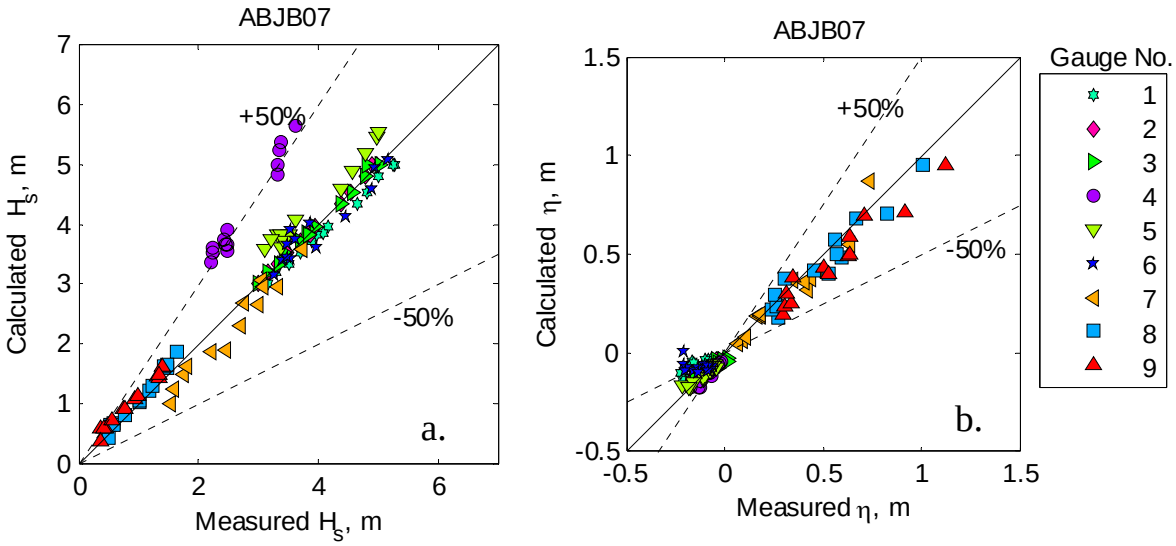

Figure 7. Comparison between measured and calculated significant wave heights (a) and average water levels (b) for the events with only wind using ABJB07.

The DDD85 model predicted wave heights over the reef face are also within 50% of the measurements (Figure 8a). Wave heights at the reef edge (Gauge 7) are underestimated and overpredicted at Gauges 8 and 9. Difference between the predicted and data over the reef top for some test conditions is greater than 50% of the measured values. Both ABJB07 and DDD85 models predict the wave setup over the reef top but fail to match wave setdown at Gauges 5 and 6..

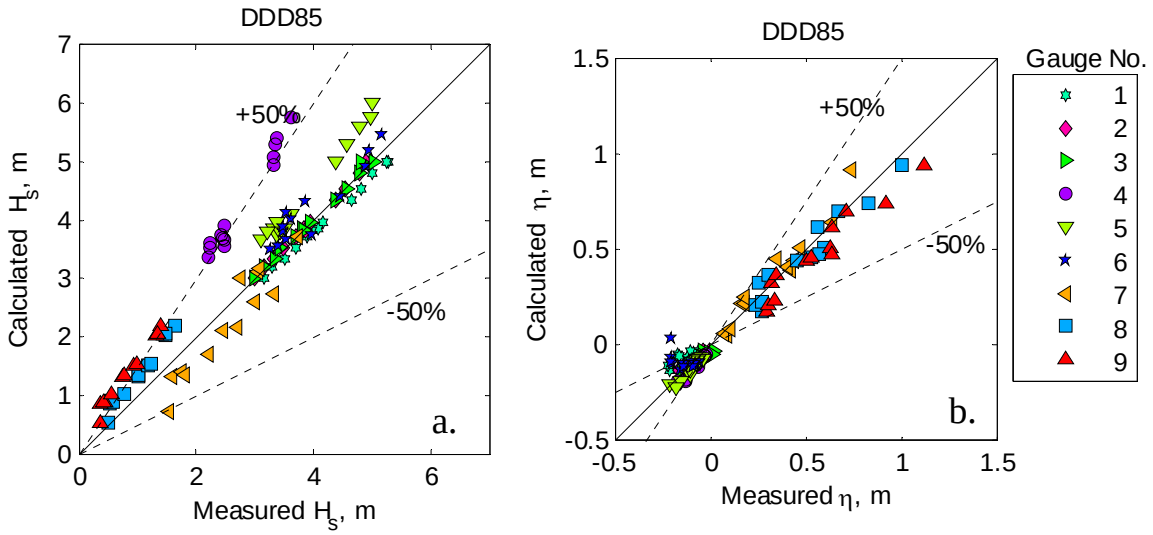

Figure 8. Comparison between measured and calculated wave heights (a) and average water levels (b) for the events with only wind using DDD85.

5.2 Tests with Waves and Wind

Figure 9 shows the comparison of measured and computed significant wave heights and mean water levels for Tests 75 and 85 with both wind and waves present. Test 75 shows a significant increase in wave height from Gauge 8 to 9 caused by the strong winds of 37.5 m/sec. The DDD85 model over predicts the wave heights on the reef face.

When wave reach the stable wave height limit in the case of DDD85 model, the wave height remains constant (without the presence of friction). Consequently, the wave setup does not change. In the ABJB07 model, a fraction of waves are breaking and this causes an increase in the wave setup over the reef top.

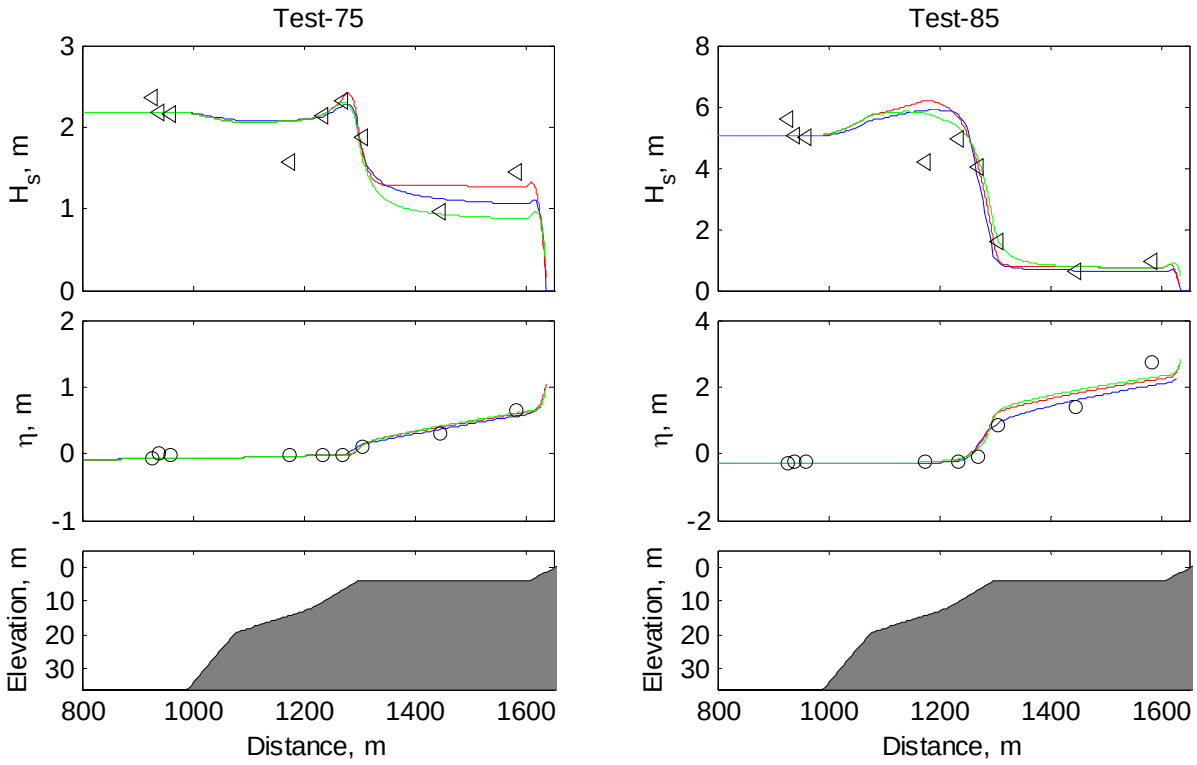

Figure 9. Comparison between measured and computed significant wave heights and mean water levels for Test 75 (H_o =2.18 m, T_p =8.0 sec, h_r =1.92 m, U =32.4 m/sec) and Test 85 (H_o =5.06 m, T_p =16.0 sec, h_r =0.0 m, U =41.4 m/sec).

— ABJB07, — DDD85, — STAD.

Gauges 2 and 3 occurs for all test conditions. Wave heights over the reef top are underestimated by STAD model especially for tests performed with shallow depths over the reef-top; see the points at the bottom portion of Figure 7a. There is not a significant difference in the wave height comparison with observations as compared to the waves only tests. The wind contribution in the STAD helps to obtain better prediction of the water surface elevations over the reef top (Figure 10b). There is a large scatter as compared to wave only tests, and the bias in water level setup is less. In general, large scatter occurs in wind-induced setup for tests with both wind and waves. The bias for combined wind and waves setup is less.

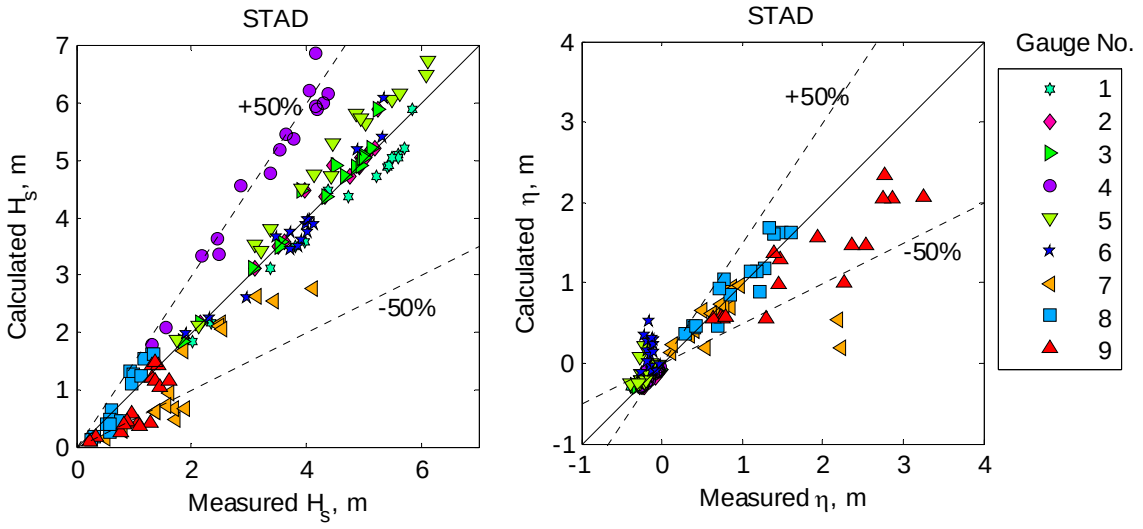

Figure 10. Comparison between measured and calculated significant wave heights for the events with both wind and waves using STAD.

Similar to the tests with only wave forcing, the ABJB07 model accurately predicted wave heights over the reef face (Gauges 4-6) and at Gauges 7 and 8 for combined wind and wave tests (Figure 11a). This could be partly due the over prediction of the setup over the reef top (Figure 11b). The over prediction of setup on reef top is caused by higher deep water waves, and if the offshore wave heights were reduced, the setup and wave heights at Gauges 7, 8 and 9 would all decrease. A poor agreement between predicted and measured wave heights is apparent at Gauge 9. Decreasing offshore wave heights would further reduce this agreement in the wave heights. The addition of wind increased the scatter in the water surface elevations as compared to the wave only tests.

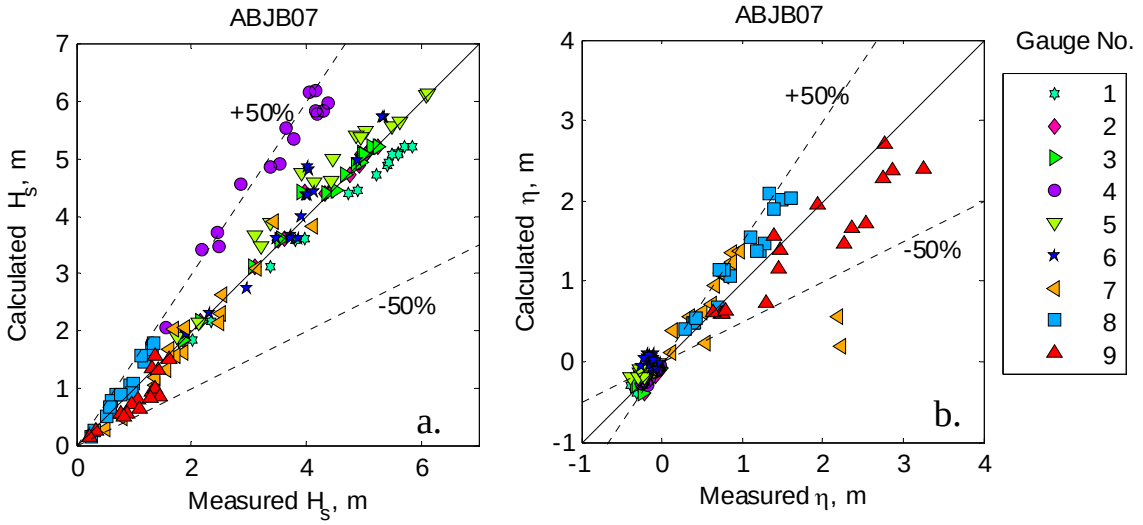

Figure 11. Comparison between measured and calculated significant wave heights (a) and average water levels (b) for the events with both wind and waves using ABJB07.

Both the STAD and DDD85 models show clustering of wave heights as a function of water depth over the reef. Since the clustering occurs also for wave only tests, this would suggest that models are limiting the calculated wave heights according to the water depth. There is an increase in the scatter between DDD85 model predicted and measured water surface elevations (Figure 12b). Both ABJB07 and DDD85 model overestimate water levels at Gauges 7 and 8, and underestimate water levels at Gauge 9.

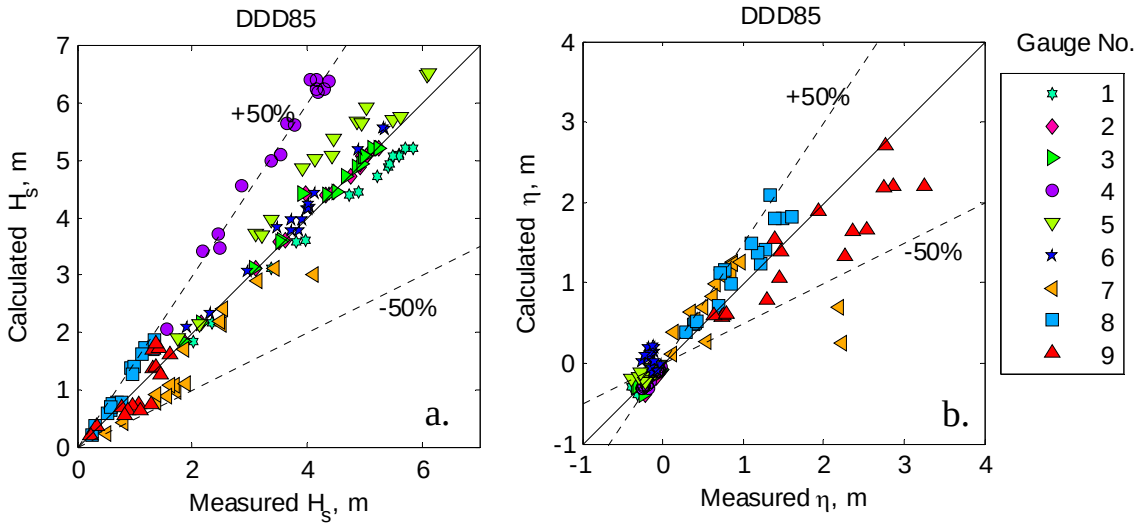

Figure 12. Comparison between measured and calculated wave heights (a) and average water levels (b) for the events with both wind and waves using DDD85.

5.3 Wind Only Tests

Figure 13 shows an example of a test case forced only by wind. This example illustrates the importance of the wind in the momentum balance in the nearshore region. Even though there was no paddle-driven wave forcing, relatively wave heights were recorded at all gauges due to wind generation of waves in the flume. As expected all three models produce almost identical average water surface elevations (assuming wind forcing only).

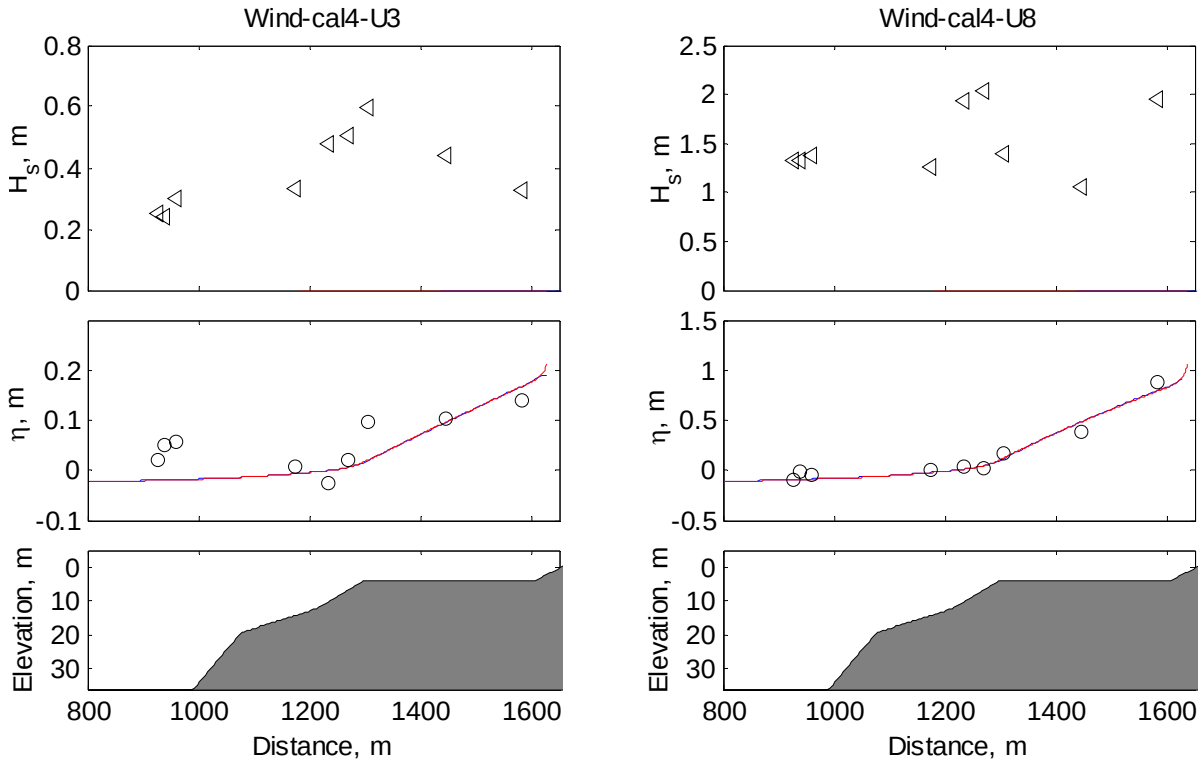

Figure 13. Comparison between measured and computed wave heights and mean water levels for test Wind-cal4-U3 (H_o =0.0 m, T_p =0.0 sec, h_r =1.02 m, U =18.5 m/sec) and Wind-cal4-U8 (H_o =0.0 m, T_p =0.0 sec, h_r =1.02 m, U =41.2 m/sec).

— ABJB07, — DDD85, — STAD.

The measured and calculated (only ADCIRC run) water surface elevations for wind only tests are compared in Figure 14a. The ADCIRC predicted values agree better with data in deepwater and for strong wind speeds, but model instabilities developed near the reef rim and continued in shallow depths on reef top for weak wind speeds. Since with the presence of waves The identical results from ABJB07 and DDD85 models are combined in Figure 18 that show water elevations are virtually the same as the ADCIRC model results except for one test in which the 1D model predicted dry conditions at Gauges 8 and 9.

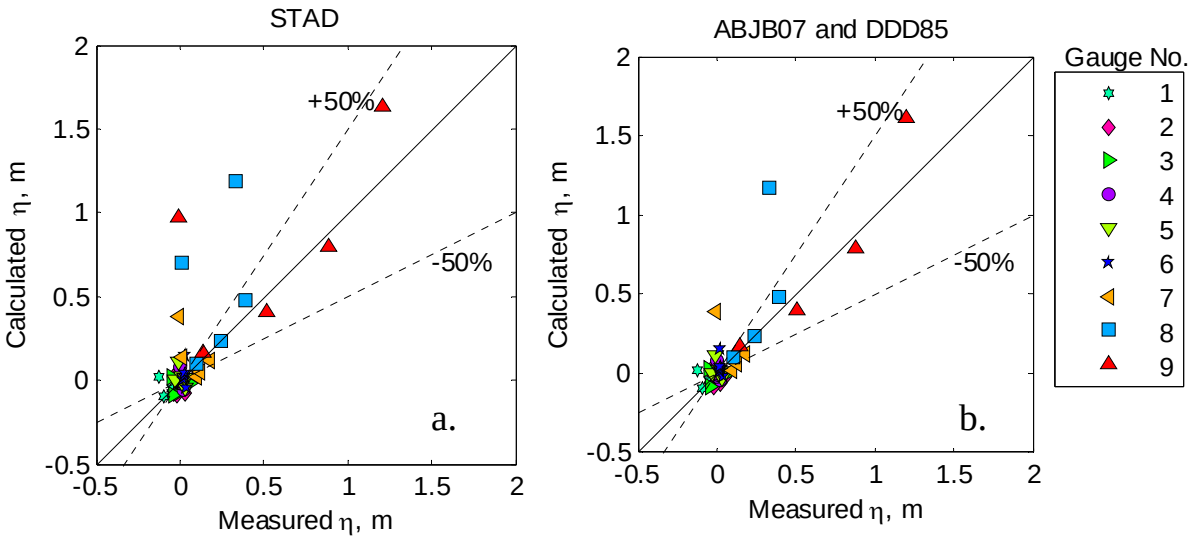

Figure 14. Comparison between measured and calculated average water levels for the events with only wind using STAD (a) and using ABJB07 and DDD85.

5.4 Summary

The performances of three different numerical model are evaluated relative to the deep-water significant wave height H_o for predictive purposes. The relative percent error is defined as $\left|x_{\text{meas}} - x_{\text{comp}}\right| / H_o$ where the subscripts meas and comp stand for measured and computed and x is either the significant wave height or the mean water level. The maximum relative percent errors for both the significant wave heights at Gauges 4 through 9 are shown in Figure 15.

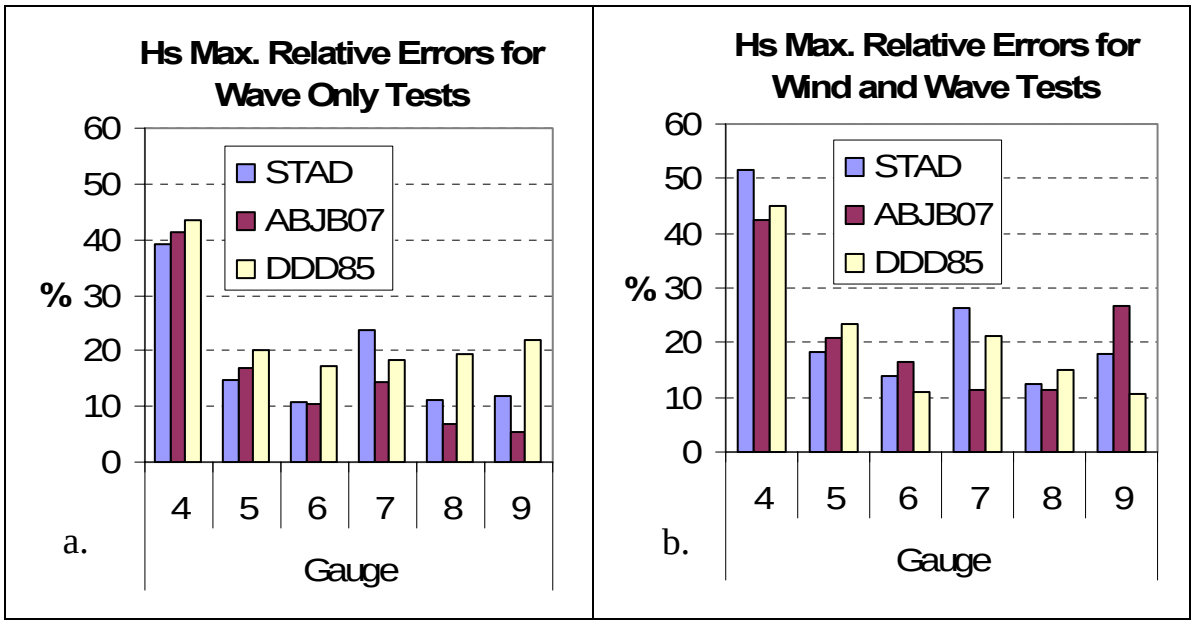

Figure 15. Significant wave height relative errors for the wave only tests (a), and wind and waves tests (b).

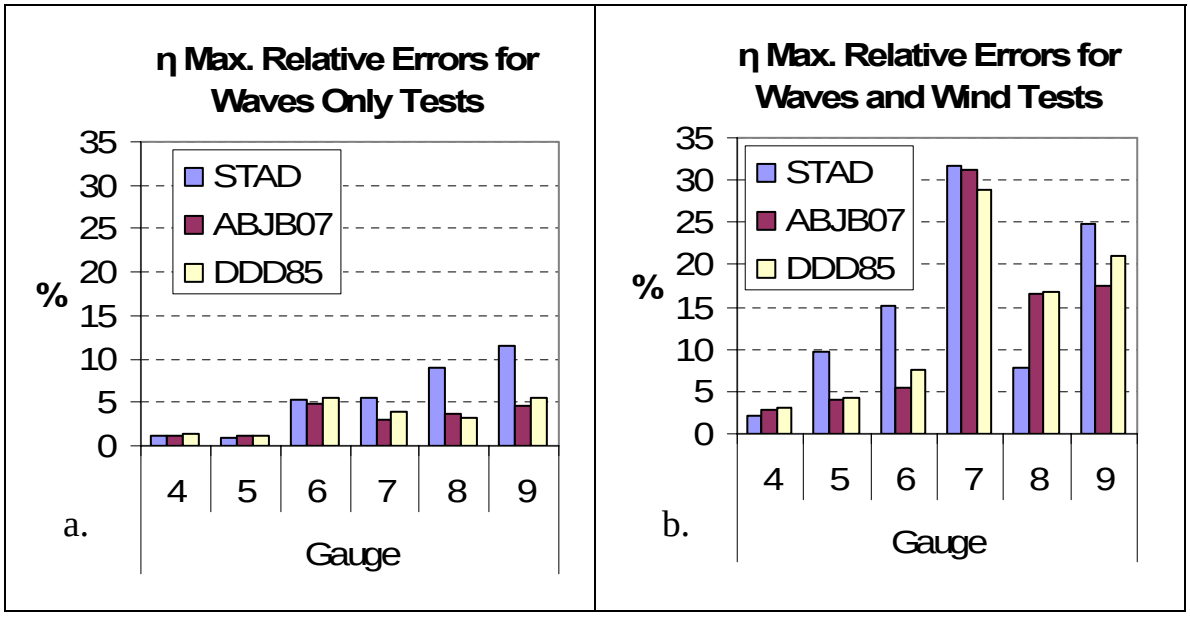

Figure 16. Significant wave height relative errors for the wave only tests (a), and wind and waves tests (b).

$$\varepsilon = \frac{1}{N}\sum_{i=1}^{N}\frac{\left|x_{\text{meas}}^{i} - x_{\text{comp}}^{i}\right|}{H_o} \tag{13}$$

where the subscripts meas and comp stand for measured and computed, x is either the significant wave height or the mean water level, i indicates the *i-th* experiment of N number of experiments.

compared in Table 1 using the Root-Mean-Squared-Error (RMSE). The ABJB07 model produced the best results for wave setup for both waves only and wind and waves combined. The coupled STWAVE and ADCIRC models produced the least accurate results for both waves only and wind and waves combined. This is likely due to the fact that the wave and setup are not solved simultaneously and only two iterations were used. Also, the resolution was somewhat courser. The accuracy of predictions by all three model decreased for tests having both wind and waves.

Table 1. Evaluation of model performance against measured significant wave height (H_s) and average water level (η), by comparison of the Root-Mean-Squared-Error (RMSE) for three models

Dataset	All		Only Waves		Waves and Wind		Only Wind
Model	H_s, m	η, m	H_s, m	η, m	H_s, m	η, m	η, m
STAD	0.620	0.268	0.548	0.120	0.673	0.344	0.244
ABJB07	0.559	0.237	0.542	0.063	0.572	0.314	0.179
DDD85	0.650	0.238	0.631	0.064	0.665	0.316	0.179

6.0 Runup

The empirical relation of Mase (1989) for the 2% runup (runup exceeded 2% of the time) for gentle slopes is given by

$$R_{2\%} = 1.86\xi^{0.71} \tag{15}$$

where ξ is the surf similarity parameter defined as $\xi = \tan\theta / \sqrt{H_o / L_o}$. On fringing reefs, waves usually break near the reef rim, may reform again over the reef top. Thus, it is logical to use the wave height over the reef top H_r in Equation (15) instead of the deep

water wave height. The wave length in the surf similarity parameter is based on peak period of waves. The water surface elevations on reef top are dominated by long period infra-gravity waves, which cannot be represented with models discussed in this paper. Therefore, the deepwater wave length had to be used in Equation (15). Figure 15 shows comparison between measured runup versus estimates from Equation (15) obtained with models ABJB07 and DDD85. The computed and measured runup values are in good agreement; calculated runup values are higher for smaller ($R_{2\%}$ <1.5 m) runup values. The model ABJB07 underestimates higher runup values since wave dissipation over the reef top is not included in the DDD85.

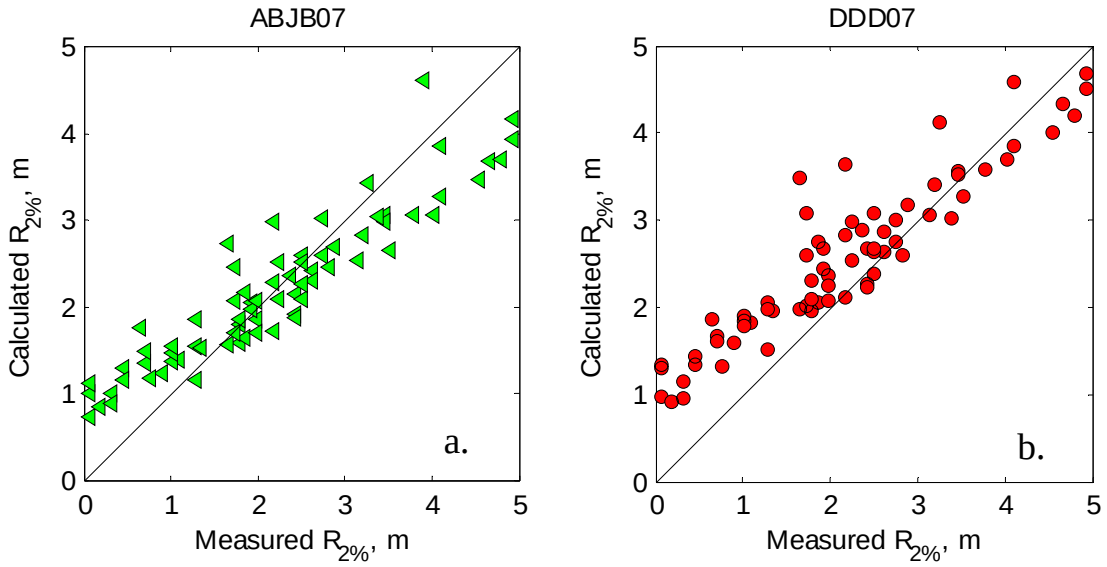

Figure 15. Comparison between measured and calculated 2% runup using Equation 15 with wave heights from ABJB07 (a) and DDD85 (b). Runup heights are respect to still-water level.

7.0 Comparison with Hayman Island Dataset

In this section, estimates from wave energy balance models ABJB07 and DDD07 are compared to the laboratory experiments of Gourlay (1994) (see Section 2.2). Measured and computed wave heights and mean water levels across the fringing reef are depicted in Figures 16 and 17. The model estimates of wave heights over the reef are fairly good; there is considerable scatter in the measurements. Both models ABJB07 and DDD85 overestimate wave setup for Tests 1.1 and 2.1 (Figure 16). Agreement is fair for Test 2.4

(Figure 17a). Seelig (1983) found that random waves of a given offshore significant wave height and period produce less setup as compared to monochromatic waves of the same wave height and period. Seelig attributed this difference in setup to the fact that irregular waves contain about half the energy of equivalent monochromatic waves. Based on this observation, the model ABJB07 should underestimate wave setup,.

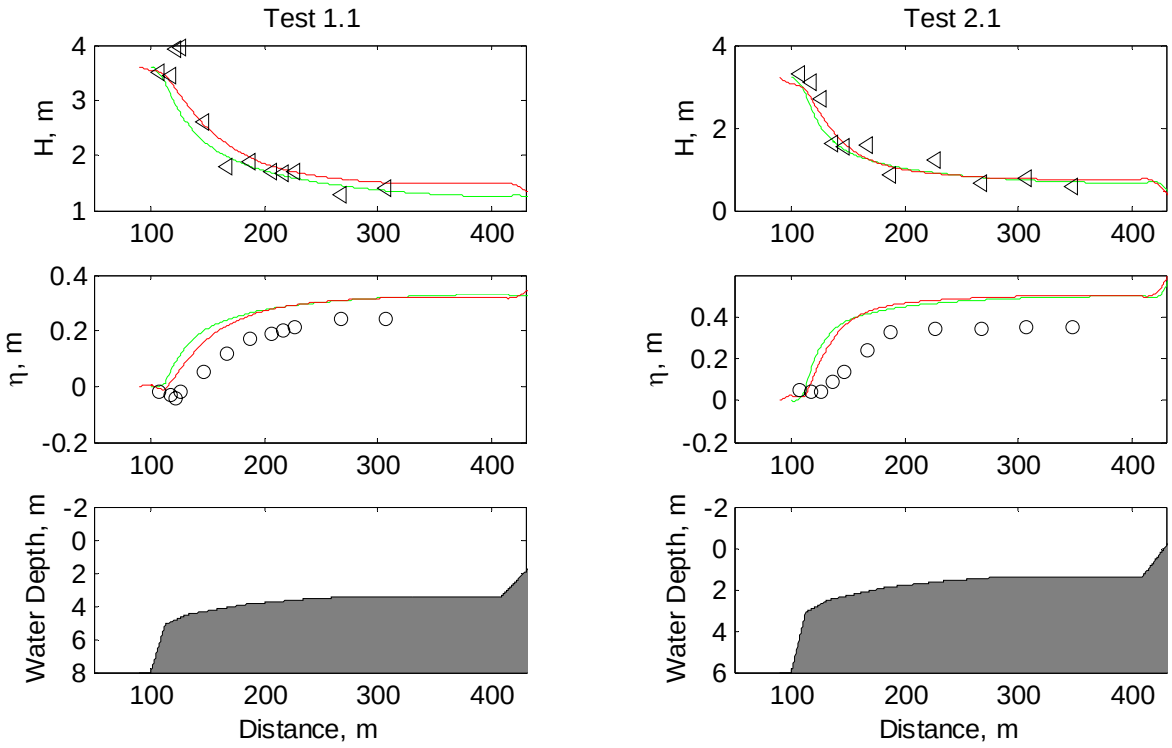

Figure 16. Comparison between measured and computed wave heights and average water levels for Test 1.1 (a) (H_i =3.44 m, T =6.8 sec, h_r =3.4 m) and 2.1 (b) (H_i =4.22 m, T =10.0 sec, h_r =1.4 m). — ABJB07, — DDD85

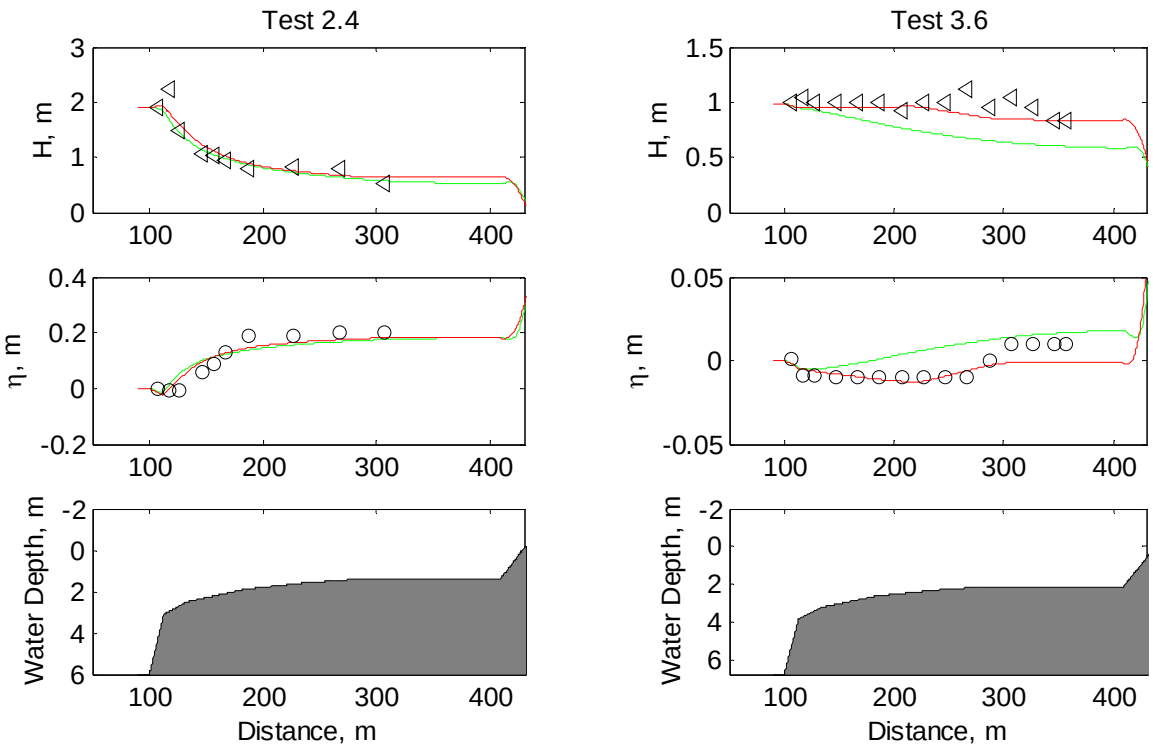

Figure 17. Comparison between measured and computed wave heights and average water levels for Test 2.4 (a) (H_i =1.90 m, T =5.4 sec, h_r =1.4 m) and 3.6 (b) (H_i =0.99 m, T =3.8 sec, h_r =2.1 m). — ABJB07, — DDD85

Measured and computed wave heights and mean water levels obtained with models ABJB07 and DDD85 are compared in Figure 19. The results of DDD85 agree better with the data for wave heights and mean water levels. The agreement is evident by the RMSE values, rms errors are 0.6887 and 0.5645 respectively for wave heights and mean water levels for model ABJB07, and for DDD85 rms errors are 0.3411 m and 0.3360 m respectively.

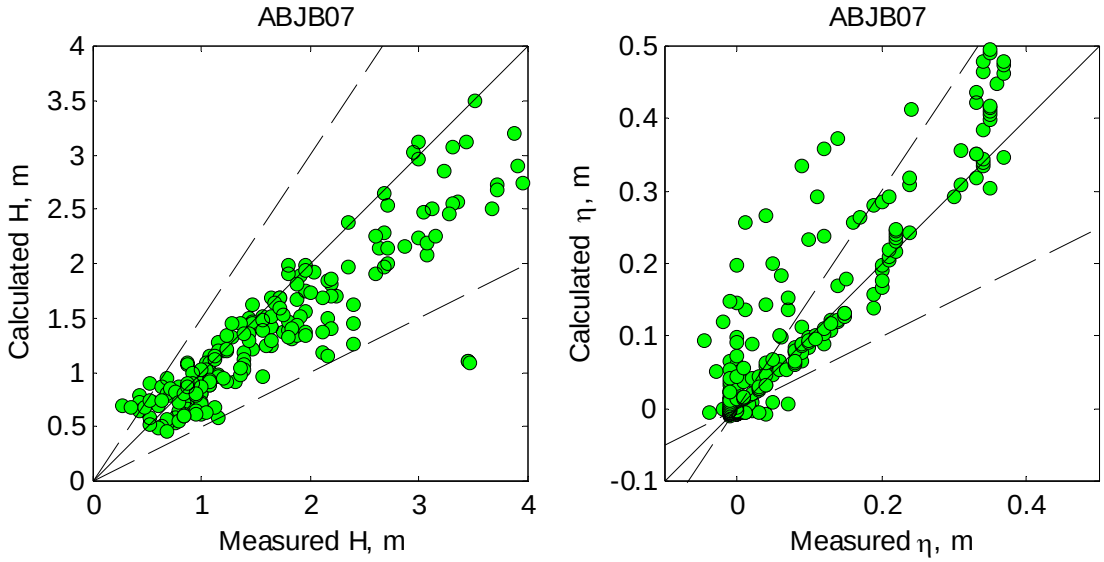

Figure 18. Comparison between measured and computed wave heights (a) and mean water levels (b) for ABJB07

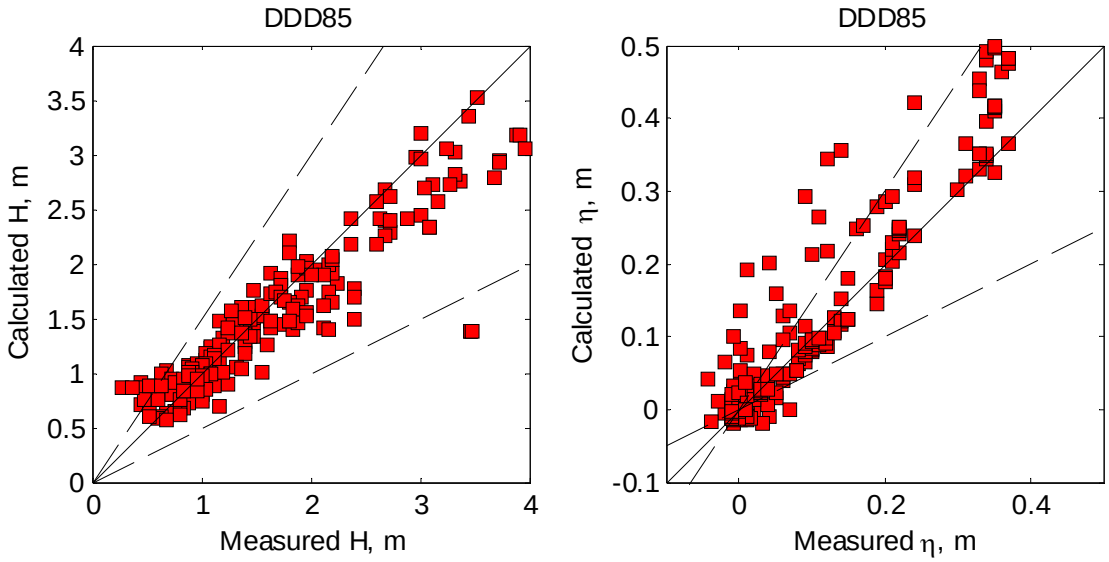

Figure 19. Comparison between measured and computed wave heights (a) and mean water levels (b) for DDD85

8.0 Discussion

The most obvious effect of the wind in the UM experiments is an apparent increase in the water level on reef top. For an onshore wind speed of the order of 10 m/s, Van Rijn and Wijnberg (1996) obtained a significant wind setup of about 0.25 m at the shoreline of a steep barred beach in Lake Michigan. Dally (1992) observed that offshore winds have a significant influence on surf zone dynamics by delaying the onset of wave breaking. Onshore winds are commonly known by suffers to induce early wave breaking. This impact is not included in the models discussed here. The laboratory measurements show that the wind setup across the reef platform give rise to larger wave heights on the reef top.

Consistent with Equation 13, the wave setup was found to increase as a function of the difference between the offshore wave height and water depth over the reef. When the waves began to break further offshore, less setup is produced. For example, by increasing the breaking intensity factor B, more energy is lost in deep water causing a smaller wave setup over the reef. Also, consistent with Equation 13, the wave setup increases with decreasing water depth over the reef and increases with wind speed.

Breaking processes over fringing reefs differ from sandy beaches. The breaking intensity is expected to be greater for fringing reefs because of their steep faces, high roughness and shallow depths. Wave attenuation rates over reefs are commonly in the range of 75-95% (e.g., Lugo-Fernandez et al. 1995; Brander et al. 2004). For the Alsina and Baldock (2007) formulation for wave breaking dissipation, the parameter B (set to 1.0 here) controls the breaking intensity. In the case of the wave breaking formulation of Dally et al. (1985) the equivalent parameter is κ (set to 0.17 here). These parameters are expected to be larger for fringing reefs. For example, further of the testing of the Alsina and Baldock (2007) formulation revealed that $B = 1.26$ produces the best agreement with the UM dataset. The parameters κ and B are expected to be a function of the breaker type. The energy dissipation due to wave breaking was also found to be inversely proportional to the incident wave period. The energy decay coefficient could be parameterized as a function of the wave period to include this effect. The wave energy decay coefficient is also expected to be a function of the breaker type (reefs are more likely to induce plunging breakers and beaches, spilling breakers).

The other free parameters in these wave breaking formulations which can be calibrated to some extent are the breaking wave height H_b in Alsina and Baldock (2007) and the

stable wave height parameter Γ in Dally et al. (1985). These parameters control the initiation and cessation of wave breaking and therefore the saturated wave heights. Laboratory measurements suggest that a stable wave height parameter Γ based on a saturated surf zone for sand beaches (Γ =0.42) and the breaking wave height according the Miche's criterion are too small for fringing reefs.

More research is needed on how to select the free parameters in the wave breaking formulations to account for different breaker types, bottom conditions and possibly wind conditions. Nonetheless, the current results show that reasonable estimates of wave height and water levels can be obtained over fringing reefs without any calibration.

The reason the STWAVE and ADCIRC models under predicted setup over the fringing reef is related to the coupling between the models and the wave breaking formulation of Battjes and Janssen (1978). In the coupling procedure, the wave model (STWAVE) is run initially using the still-water level and computes the wave radiation stress gradients which are then used to force the flow (ADCIRC). These wave radiation stress gradients are under predicted because the setup is not initially considered in the wave model. The results suggest that more than one iteration between the models is needed to accurately model the wave setup over a fringing reef. For real life application, this also suggests that special attention is needed to the coupling between the models when the wave conditions and water levels are varying rapidly with time and space, such as in the tropical storm and on reefs to avoid similar problems.

The second laboratory dataset used consisted of the monochromatic waves over a fringing reef profile typical to that of Hayman Island (Gourlay 1994). The 1D wave energy balance models were applied to this dataset and produced reasonable agreement with laboratory measurements. The offset of the computed wave setdown with respect to measurements indicates that the wave breaking would be better represented by a roller type formulation for wave breaking (Stive and De Vriend 1994). However, the models still calculate the wave heights and water elevations within a 50% error.

9.0 Conclusions and Recommendations

Computed wave heights and water levels from two 1D wave energy balance models with difference wave breaking formulations and the coupled STWAVE and ADCIRC models were compared with laboratory measurements of combined wind and waves over a

fringing reef profile typical of the Island of Guam (Demirbilek et al. 2007a). The three approaches produce results which are in good agreement with laboratory measurements.

The parametric models, although not intended for quantitative purposes, provide good qualitative results within a maximum percent error of 50%. These models are intended for practical applications and not to study the wave mechanics over coral reefs. These models constitute a useful for tool emergency management and structure design and other engineering applications.

The most important effect of the wind over coral reefs is the wind setup which allows the waves to rebuild and increase in height. Due to the shallow depths over fringing coral reefs, the wind contribution to the setup may be as large as the wave setup especially for strong winds and wide reef tops.

Acknowledgements. Permission to publish this paper was granted by the Office, Chief of Engineers, U.S. Army Corps of Engineers. This research was supported by the Surge and Wave Island Modeling Studies Program.

References

Alsina, J.M. and Baldock, T.E. (2007) Improved representation of breaking wave energy dissipation in parametric wave transformation models, *Coastal Engineering*, 54, 765-769.

Battjes, J.A., Janssen, J.P.F.M (1978) Energy loss and set-up due to breaking of random waves, *Proceedings Coastal Engineering*, ASCE, pp. 569-587.

Brander, R.W., Kench, P.S., Hart, D. (2004) Spatial and temporal variations in wave characteristics across a reef platform, Warraber Island, Torres Strait, Australia, *Marine Geology*, 207, 169-184.

Dally, W.R., Dean, R.G., and Dalrymple, R.A. (1985) Wave height variation across beaches of arbitrary profile, *Journal of Geophysical Research*, 90(C6), 11917-11927.

Dally, W.R. (1992) Random breaking waves: field verification of a wave-by-wave algorithm for engineering applications, *Coastal Engineering*, 16, 369-397.

Demirbilek, Z., Nwogu, O.G. and Ward, D.L. (2007a) Laboratory study of wind effect on runup over fringing reefs, ERDC/CHL TR-07-04. Vicksburg, MS: U.S. Army Engineer Research and Development Center, Coastal and Hydraulics Laboratory.

Demirbilek, Z. and Nwogu, O.G. (2007b) Boussinesq modeling of wave propagation and runup over fringing coral reefs, ERDC/CHL TR-XX-XX. Vicksburg, MS: U.S. Army Engineer Research and Development Center, Coastal and Hydraulics Laboratory.

Douglass, S.L**.** (1990) Influence of Wind on Breaking Waves, *Journal of Waterway, Port, Coastal and Ocean Engineering*, ASCE. WW6, 116, 651-663.

Gerritsen, F. (1980) Wave attenuation and wave setup on a coastal reef. *Proceedings 17th International Conference on Coastal Engineering*, Sydney, Australia. New York, ASCE, 444-461.

Gerritsen, F. (1981) Wave attenuation and wave setup on a coastal reef, University of Hawaii, Look Laboratory, Technical Report No. 48, pp. 416.

Gourlay, M. R. (1996a) Wave set-up on coral reefs. 1. Set-up and wave-generated flow on an idealized two dimensional horizontal reef. *Coastal Engineering* 27, 161-193.

Gourlay, M. R. (1996b) Wave set-up on coral reefs. 2. Set-up on reefs with various profiles, *Coastal Engineering,* 28, 17-55.

Gourlay, M.R. (2005) Wave-generated flow on coral reefs-an analysis for two-dimensional horizontal reef-tops with steep faces, *Coastal Engineering*, 52, 353-387.

Grasmeijer, B.T. and Ruessink, B.G. (2003) Modeling of waves and currents in the nearshore: parametric vs. probabilistic approach, *Coastal Engineering*, 49, 185-207.

Janssen, T.T. and Battjes, J.A. (2007) A note on wave energy dissipation over steep beaches, *Coastal Engineering*, 54, 711-716.

Larson, M., and Kraus, N.C. (1991) Numerical model of longshore current for bar and trough beaches, *Journal of Waterway, Port, Coastal, and Ocean Engineering*, 117(4), 326-347.

Longuett-Higgins, M.S. and Stewart, R.W. (1964) Radiation stress in water waves: A physical discussion with applications, *Deep Sea Research*, 11.

Luettich, R. A., Westerink, J. J., and Scheffner, N. W. (1992) ADCIRC: An advanced three-dimensional circulation model for shelves, coasts, and estuaries; Report 1, theory and methodology of ADCIRC-2DDI and ADCIRC-3DL, ERDC/CHL TR DRP-92-6, Vicksburg, MS: U.S. Army Engineer Waterways Experiment Station, Vicksburg, MS.

Lugo-Fernandez, A., Roberts, H.H. and Suhayada, J.N. (1998) Wave transformation across a Caribbean fringing-barrier coral reef, *Continental Shelf Research*, 18, 1099-1124.

Mase, H. (1989) Random wave runup height on gentle slope, *Journal of Waterway, Port, Coastal and Ocean Engineering*, 115(5),649-661.

Massel, S.R., and Gourlay, M.R. (2000) On the modeling of wave breaking and set-up on coral reefs, *Coastal Engineering*, 39, 1-27.

Miche, M. (1951) Le pouvoir reflechissant des ouvrages maritimes exposes a l'action de la houle. Annals des Ponts et Chaussessm 12le Anne, 2850319 (translated by Lincoln and Chevron, University of California, Berkeley, Wave Research Laboratory, Series 3, Issue 363, June 1954).

Nwogu, O. (2006) Personal communication with Edward Thompson, University of Michigan, Department of Architecture and Marine engineering, Ann Arbor, MI 48109.

Ruessink, B.G., Walstra, D.J.R., Southgate, H.N. (2003) Calibration and verification of a parametric wave model on barred beaches. Coastal Engineering, 48 (3), 139–149.

Sánchez, A., Smith, J.M., Demirbilek, Z, Boc, S. (2007) User's manual to the Coastal Modeling Package – TWAVE, Unpublished Letter Report, Vicksburg, MS, U.S. Army Engineer and Research Development Center.

Seelig, W.N. (1983) Laboratory Study of Reef-Lagoon System Hydraulics, *Journal of Waterway, Port, Coastal and Ocean Engineering*, ASCE, 109(4), 380-391.

Smith, J.M. (1993) Nearshore wave breaking and decay, ERDC/CHL TR-93-11, Vicksburg, MS: U.S. Army Engineer Research and Development Center, Coastal and Hydraulics Laboratory.

Smith, J.M., Sherlock, A.R., Resio, D.T. (2001) STWAVE: Steady-State Spectral Wave Model: user's manual for STWAVE, Version 3.0, ERDC/CHL SR-01-01, Vicksburg,

MS: U.S. Army Engineer Research and Development Center, Coastal and Hydraulics Laboratory.

Stive, M.J.F. and De Vriend, H.J. (1994) Shear stresses and mean flow in shoaling and breaking waves, Proceedings Coastal engineering, ASCE, New York, pp. 594-608.

Thornton, E. B., and Guza, R. T. (1983) Transformation of Wave Height Distribution, *Journal of Geophysical Research*, 88(C10), 5925-5938.

Thompson, E.F, and Scheffner N.W. (2002) Typhoon-induced stage-frequency and overtopping relationships for the commercial port road, Territory of Guam, ERDC/CHL TR 02-01, Vicksburg, MS: U.S. Army Engineer Research and Development Center, Coastal and Hydraulics Laboratory.

Thompson, E.F. (2005) A physical model study for investigation of wave processes over reefs, Coastal Hydraulics Laboratory, Unpublished Letter Report, Vicksburg, MS, U.S. Army Engineer and Research Development Center.

Van Rijn, L.C. and Wijnberg K.M. (1996) One-dimensional modeling of individual waves and wave-induced longshore currents in the surf zone, *Coastal Engineering*, 28, 121-145.

Van Rijn, L.C., Walstra D.J.R., Grasmeijer, B., Sutherland, J., Pan, S. and Sierra, J.P. (2003) The predictability of cross-shore bed evolution of sandy beaches at the time scale of storms and seasons using process-based Profile models, *Coastal Engineering*, 47 (3), 295–327.